TÜBİTAK

Turkish Journal of Physics

http://journals.tubitak.gov.tr/physics/

Research Article

Turk J Phys
(2015) 39: 128 – 136

doi:10.3906/fiz-1408-6

A computational study on the interaction between O_2 and pristine and Ge-doped aluminum phosphide nanotubes

Mahdi REZAEI-SAMETI*, Alireza KAZEMI
Department of Physical Chemistry, Faculty of Science, Malayer University, Malayer, Iran

Received: 20.08.2014 • **Accepted/Published Online:** 17.03.2015 • **Printed:** 30.07.2015

Abstract: In this research the interaction between oxygen molecules and the outside and inside surfaces of pristine and Ge-doped (4,4) armchair and (6,0) zigzag models of aluminum phosphide nanotubes (AlPNTs) was systematically investigated using density function theory. Structural parameters, adsorption energy, quantum parameters, HOMO/LUMO orbitals, and nuclear quadrupole resonance (NQR) parameters were calculated for all models of AlPNTs. The aim of this work was to investigate the effects of Ge doping and O_2 adsorption on the electrical and structural parameters of (4,4) armchair and (8,0) zigzag models of AlPNTs. The results revealed that adsorption energies for all models were negative with exothermic chemical bonding. By doping Ge in spite of the B52 site of (4,4) armchair and (6,0) zigzag models the adsorption energy increased significantly from pristine values and therefore Ge doping increased the reactivity of the nanotubes to O_2 adsorption. The NQR results showed that in AlPNTs Al atoms at the edges of nanotubes played a significant role in determining the electronic behaviors of AlPNTs and the average values of C_Q (^{27}Al) and η_Q for the O_2 attached on (4,4) armchair and (6,0) zigzag AlPNTs were higher than those of the pristine model. Analysis of the electronic properties indicated that adsorption of O_2 reduced the energy gap of AlPNTs. Quantum molecular results showed that the global hardness (η) of Ge-doped models was smaller than that of other models.

Key words: O_2 interaction, DFT, Ge-doped, HOMO/LUMO orbital, NQR, AlPNTs

1. Introduction

Since the discovery and synthesis of single-walled carbon nanotubes and boron nitride nanotubes [1–3], much research has been done on the properties and applications of new nanotubes made from the other elements of the third and fifth groups of the periodic table of elements by experimental technique and theoretical approach. These materials have unique and fascinating electrical, optical, chemical, thermal, and optoelectrical properties, and have wide potential applications [4–12]. Moreover, many experimental and theoretical investigations have been carried out on the tubular properties and the potentially very large adsorptive capacity of nanotubes, making them promising candidates for use in gas storage and gas sensor applications [13–15]. Recent investigations show that these novel materials can be used for studying different kinds of physisorption and chemisorption, in chemical sensors, and in electronic devices for various gases such as H_2, O_2, O_3, Cl_2, CO, NO, NH_3, N_2O, NO_2, and H_2O [16–20]. The detection of oxygen gas is important in confined spaces such as mines, pressure vessels, and aircraft where people work or travel. O_2 detectors are also used in order to detect oxygen in some chemical manufacturing processes. So far, a few O_2 sensors based on nanotubes have been developed [21–23].

*Correspondence: mrsameti@gmail.com

The effects of oxygen adsorption on single wall nanotubes of zigzag and armchair models with relatively large diameters have already been reported experimentally and theoretically [24–26]. The results show that the process of oxygen adsorption on nanotubes can be exothermic or endothermic [27–30]. Some of these studies have focused on the physisorption of O_2, while others have considered both physisorption and chemisorption [31–33]. Following our previous work on the structures and electrical and NMR parameters of SiC-doped aluminum phosphide nanotubes (AlPNTs), Ga-doped boron phosphide nanotubes (BPNTs), Al- and N-doped BPNTs, and Ge- and As-doped BPNTs [34–37], in the present research we investigated the sensitivity of undoped and Ge-doped AlPNTs toward O_2 molecules using density functional theory. The structural parameters, adsorption energy, quantum parameters, HOMO/LUMO orbitals, and NQR parameters for adsorption of O_2 on the outside and inside of undoped and Ge-doped (4,4) armchair and (6,0) zigzag models of AlPNTs were calculated.

2. Computational methods

The structural and electrical properties of adsorption of O_2 gas on the outer and inner surfaces of pristine and Ge-doped (4,4) armchair and (6,0) zigzag models of AlPNTs (see Figures 1 and 2) were investigated by density function theory, at B3LYP level of theory, and 6-31G(d) base set using the Gaussian 03 set of programs [38,39]. In this work, we considered four models (A–D) for adsorption of O_2 gas on the surface of nanotubes: Model A shows the vertical adsorption of O_2 gas on the outer surface of AlPNTs, Model B indicates the vertical adsorption of O_2 gas on the inner surface of AlPNTs, Model C shows the parallel adsorption of O_2 gas on the outer surface of AlPNTs, and Model D demonstrates the parallel adsorption of O_2 gas on the inner surface of AlPNTs (see Figures 1 and 2). After optimizing the structures of all the considered nanotubes in this study, we calculated the adsorption energy (E_{ads}) of oxygen on the pristine and Ge-doped AlPNTs models as follows:

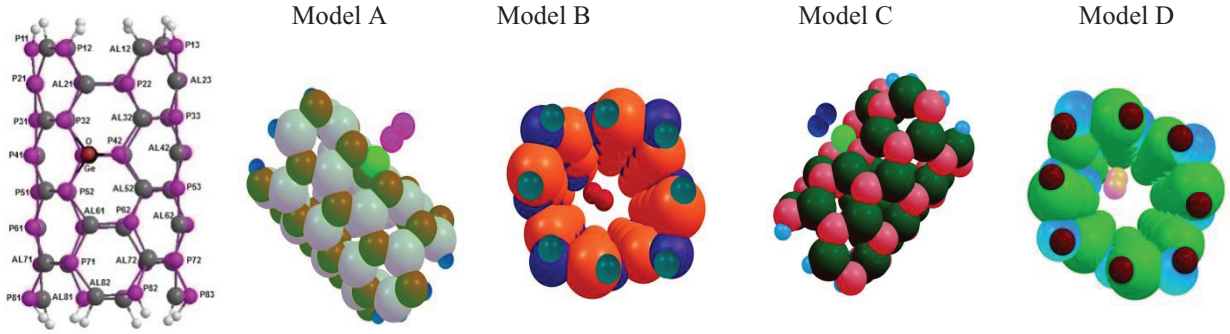

Figure 1. 2D views of O_2 adsorption on the (4,4) armchair model of AlPNTs for A–D models.

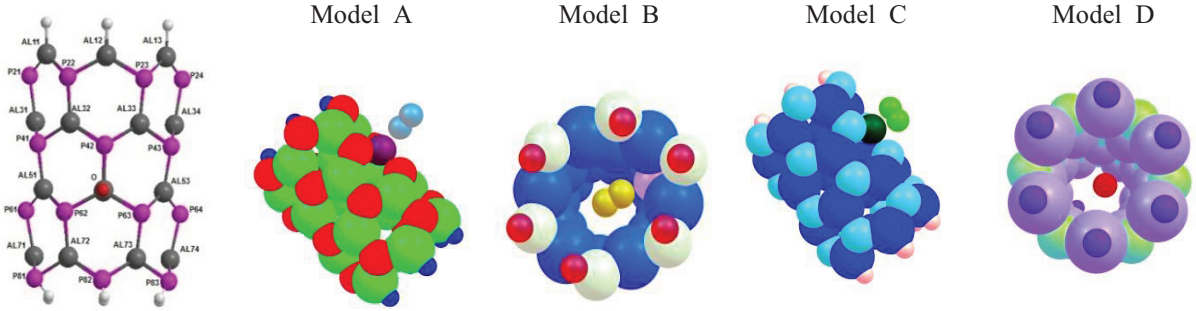

Figure 2. 2D views of O_2 adsorption on the (6,0) zigzag model of AlPNTs for A–D models.

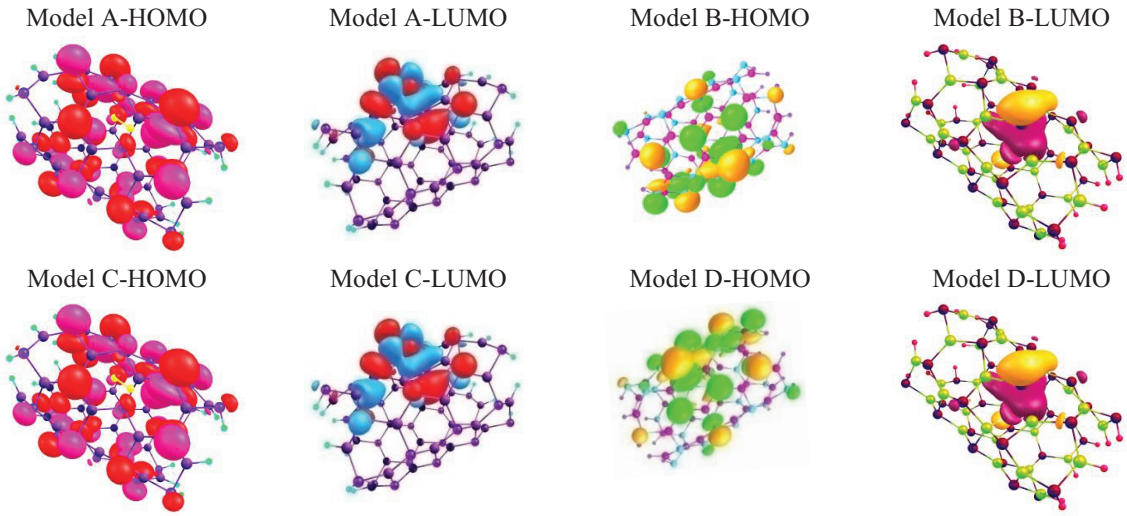

Figure 3. Comparisons the HOMO and LUMO structures of adsorption O_2 gas on surface of (4,4) armchair AlPNTs for A–D models.

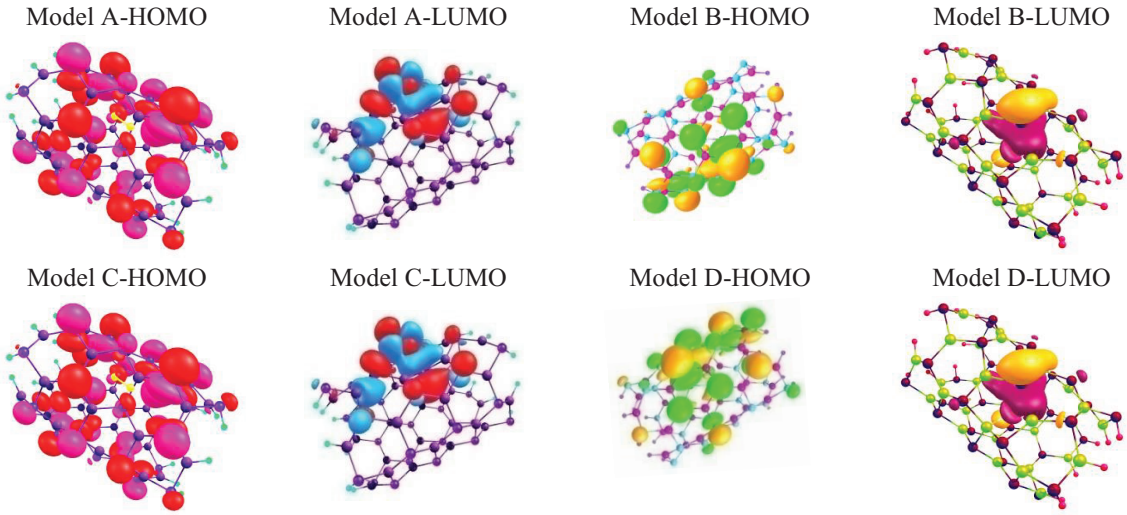

Figure 4. Comparisons the HOMO and LUMO structures of adsorption O_2 gas on surface of (6,0) zigzag AlPNTs for A–D models.

$$E_{ads} = E_{AlPNTs-O_2} - (E_{AlPNTs} + E_{O_2}) + BSSE, \tag{1}$$

where $E_{AlPNTs-O2}$ is obtained from the scan of the potential energy of the AlPNTs–O_2 complex, E_{AlPNTs} is the energy of the optimized AlPNTs structure, E_{O2} is the energy of an optimized O_2, and BSSE stands for base set superposition errors. Quantum molecular descriptors, i.e. electronic chemical potential (μ), global hardness (η), electrophilicity index (ω), energy gap, global softness (S), and electronegativity (χ), of nanotubes were calculated as follows:

$$E_{gap} = E_{HOMO} - E_{LUMO} \tag{2}$$

$$\eta = (I - A)/2 \tag{3}$$

$$\mu = -(I + A)/2 \tag{4}$$

$$\chi = -\mu \tag{5}$$

$$\omega = \mu^2/2\eta \tag{6}$$

$$S = 1/2\eta, \tag{7}$$

where I (-E$_{HOMO}$) is the ionization potential and A (-E$_{LUMO}$) is the electron affinity of the molecule. The electrophilicity index is a measure of the electrophilicity power of a molecule [40–42]. The quadrupole coupling constants (C_Q) and asymmetry parameters (η_Q) are measured by nuclear quadrupole resonance (NQR).C_Q refers to the interaction energy of the nuclear electric quadrupole moment, (e_Q), and the electrical field gradient (EFG) tensors at the site of a quadrupole nucleus. Quantum chemical calculations yield principal components of the EFG tensor, q_{ii}, in atomic unit 1 au = 9.717365 $\times$ 1021 V m^{-2}, with $q_{zz} > q_{yy} > q_{xx}$. Eqs. (8) and (9) are used to relate the calculation of EFG tensors with the measurable parameters of C$_Q$ and η_Q. The standard Q value as reported by Pyykkö [43] is (Q ^{27}Al) =146/61 mb.

$$C_Q(MHZ) = e^2 Q q_{zz} h^{-1} \tag{8}$$

$$\eta_Q = |(q_{xx} - q_{yy})/q_{zz}| \, (q_{zz} > q_{yy} > q_{xx}) 0 < \eta_Q < 1 \tag{9}$$

3. Results and discussion

3.1. Structure parameters

In this project, all the representative adsorption structures of the models (A–D) were successfully optimized by DFT method, at the theoretical level of B3LYP, and the basis set of 6-31G (d), and the results are shown in Figures 1 and 2. The optimized results show that the average bond length (Al–P) was 2.33 Å, which is in agreement with other studies [34,44]. The comparison of results revealed similar bond lengths for equivalent positions in the pristine and Ge-doped models of AlPNTs. However, in the Ge-doped region, this similarity was interrupted. In all the models, by doping of the B52 site in (4,4) armchair and (6,0) zigzag AlPNTs with Ge atom the bond length of the atoms of the neighbor of the doped region increased while their bond angle decreased. On the other hand, the adsorption of O$_2$ gas on the outer and inner surfaces of AlPNTs slightly changed the bond length and bond angle of the neighbors of the adsorbing position.

The adsorption energy (E$_{ads}$) was calculated by using Eq. (1) and the results of the adsorption models (A–D) are summarized in Tables 1 and 2. The adsorption energies indicated that the chemical interaction between the O$_2$ molecules and the AlPNTs was weak and its bond character was physisorption. For all models, the calculated adsorption energies were negative with exothermic chemical bonding. The low energy gain was an indication of a physisorption process. For each tube molecule, it can be seen that the adsorption energies of the interactions for the A, B, C, and D models of pristine (4,4) armchair AlPNTs were about –31.90, –33.81, –33.10, and –33.84 kcal/mol, respectively, and for these models of pristine (6,0) zigzag AlPNTs were about –26.16, –26.41, –25.80, and –26.91 kcal/mol, respectively. The results showed that by doping Ge in all models the adsorption energy significantly increased from pristine values and therefore adsorption of O$_2$ gas on the surface of Ge-doped nanotubes was more favorable than that of pristine ones. The comparison of results showed that the adsorption energies for the outer and inner surfaces of the nanotubes were nearly the same. The comparison results of adsorption energy between AlPNTs and silicon nanotubes [45,46] showed that the adsorption of O$_2$ gas on the surface of AlPNTs was better than that on silicon nanotubes and was exothermic.

Table 1. Quantum parameters of O_2 adsorption on undoped and Ge doped (A–D) models (4,4) armchair model AlPNTs.

Property	Pristine		Model A		Model B		Model C		Model D	
	Undoped	Ge-doped	Undoped	Ge-doped	Undoped	Ge-doped	Undoped	Ge-doped	Undoped	Ge-doped
E_{ads}/kcal mol^{-1}	−−−	−−−	−31.90	−38.24	−33.81	−37.24	−33.1	−38.22	−33.84	−37.08
E_{HOMO}/ev	−6.29	−5.95	−6.60	−6.58	−6.51	−5.81	−6.50	−6.59	−6.52	−6.32
E_{LUMO}/ev	−2.93	−2.88	−5.18	−3.03	−3.99	−3.88	−3.66	−2.98	−3.99	−3.01
E_{gap}/ev	3.36	3.07	1.42	3.55	2.52	1.93	2.83	3.61	2.53	3.31
I/ev	6.29	5.95	6.60	6.58	6.51	5.81	6.50	6.59	6.52	6.32
A/ev	2.93	2.88	5.18	3.03	3.99	3.88	3.66	2.98	3.99	3.01
μ/ev	−4.61	−4.41	−5.89	−4.81	−5.25	−4.84	−5.08	−4.78	−5.26	−4.66
S/ev	0.29	0.32	0.70	0.28	0.39	0.51	0.35	0.27	0.39	0.30
W/ev	6.34	6.35	14.36	6.51	10.95	9.14	9.09	6.38	10.94	6.57
η/ev	1.68	1.53	0.71	1.77	1.26	0.96	1.41	1.80	1.26	1.65
X/ev	4.61	4.41	5.89	4.81	5.25	4.84	5.08	4.78	5.26	4.66

Table 2. Quantum parameters of O_2 adsorption on undoped and Ge doped (A–D) models of (6,0) zigzag AlPNTs.

Property	Pristine		Model A		Model B		Model C		Model D	
	Undoped	Ge-doped	Undoped	Ge-doped	Undoped	Ge-doped	Undoped	Ge-doped	Undoped	Ge-doped
E_{ads}/kcal mol^{-1}	−−−	−−−	−26.16	−29.95	−26.41	−31.91	−25.8	−29.18	−26.91	−34.67
E_{HOMO}/ev	−6.40	−5.85	−6.64	−6.77	−6.56	−6.66	−6.54	−5.44	−6.53	−6.54
E_{LUMO}/ev	−3.41	−3.33	−4.26	−3.66	−4.21	−3.52	−3.85	−3.61	−3.98	−3.43
E_{gap}/ev	2.99	2.52	2.37	3.11	2.35	3.14	2.68	1.83	2.54	3.11
I/ev	6.40	5.85	6.64	6.77	6.56	6.66	6.54	5.44	6.53	6.54
A/ev	3.41	3.33	4.26	3.66	4.21	3.52	3.85	3.61	3.98	3.43
μ/ev	−4.90	−4.59	−5.45	−5.21	−5.38	−5.09	−5.20	−4.52	−5.26	−4.98
S/ev	0.33	0.39	0.42	0.32	0.42	0.31	0.37	0.54	0.39	0.32
W/ev	8.03	8.36	12.52	8.75	12.32	8.26	10.0	9.17	10.86	7.98
η/ev	1.49	1.26	1.18	1.55	1.17	1.57	1.34	0.91	1.27	1.55
X/ev	4.90	4.59	5.45	5.21	5.38	5.09	5.20	4.52	5.26	4.98

3.2. Quantum molecular descriptor

To understand the nature of the interaction between O_2 gas and pristine and Ge-doped (4,4) armchair and (6,0) zigzag models of AlPNTs, the highest occupied molecular orbital (HOMO) and the lowest unoccupied molecular orbital (LUMO) in the (A–D) undoped and Ge- doped models of AlPNTs were calculated, and all structures' results are given in Figures 3 and 4. The electronic charge density of the HOMO orbital in A and B models of (4,4) armchair AlPNTs was located at the fourth layer of nanotubes. The density of the HOMO orbital in C and D models of (4,4) armchair and A–D models of (6,0) zigzag models was located at the first layer on the phosphorus atoms of nanotubes and corresponded to the lone pair of electrons on phosphorus atoms.

However, the electronic charge densities of the LUMO orbital in all models of (4,4) armchair and (6,0) zigzag models of AlPNTs were located on the B sites of nanotubes around the O_2 adsorption position (see Figures 3 and 4). The energy gap between the HOMO and LUMO orbital (E_{gap}) of the nanotube was calculated by Eq. (1) and the results are given in Tables 1 and 2. The energy gap of the nanotube can evaluate the reactivity of the chemical adsorption and electronic property of two species. Therefore, the E_{gap} of the intrinsic pristine (4,4) armchair and (6,0) zigzag models of AlPNTs were found to be 3.36 and 2.99 eV, respectively. By doping

with Ge the E_{gap} of armchair and zigzag models decreased significantly to 3.07 and 2.52 eV, respectively. It is notable that with the adsorption of O_2 in pristine model A and Ge-doped (4,4) armchair model B the E_{gap} significantly decreased to 1.43 and 1.93 eV, respectively. In the Ge-doped (6,0) zigzag model C the E_{gap} significantly decreased to 1.83 eV, and in the other models the E_{gap} decreased and increased slightly from original values. The decline in the energy gap can prove that the chemical activity of complex AlPNTs/O_2 has increased and hence the chemical stability of the nanotube will decrease.

The quantum molecular descriptors of all adsorption models (4,4) armchair and (6,0) zigzag AlPNTs were calculated by Eqs. (3)–(7) and the results are given in Tables 1 and 2. Global hardness (η) is defined as a resistance to deformation in the presence of an electric field that can increase with stability and can decrease with the reactivity of the species. The average global hardness for pristine (4,4) armchair was 1.68 eV and 1.49 eV for (6,0) zigzag models and for Ge-doped models it was 1.53 and 1.26 eV. The results indicated that the global hardness (η) of Ge-doped models was lower than that of other models.

The calculated results showed that with adsorption of O_2 gas on the surface of nanotubes the global hardness of the pristine model A and model B of Ge-doped (4,4) armchair significantly decreased to 0.71 and 0.96 eV, respectively. Moreover, the global hardness of models A and B of undoped and model C of Ge-doped (6,0) zigzag significantly decreased from the original values. The comparison of the results showed that by doping of Ge and adsorbing O_2 gas the global hardness decreased and therefore the stability of nanotube decreased, which can increase the reactivity of the species.

However, the electronegativity (χ) of A, B, and D models of undoped armchair and zigzag is larger than that of other models. These results demonstrate that electrons will flow from a definite occupied orbital in a Ge atom of AlPNTs and will go into a definite empty orbital in O_2 gas. The electrophilicity index (ω) of Ge-doped models of (4,4) armchair and (6,0) zigzag models was lower than that of all undoped models. Therefore, the maximum flow of electrons takes place from the Ge atom (as donor atom) to nanotube (as acceptor species), which supplies the structural stability and reactivity of the nanotube complex.

3.3. NQR parameters of ^{27}Al

In this work, to study the effect of Ge doping and O_2 adsorption on the (4,4) armchair and (6,0) zigzag models of AlPNTs, the NQR parameters at the sites of various ^{27}Al nuclei were calculated and the results are given in Tables 3 and 4. The NQR parameters were divided into four layers based on the likeness of the calculated EFG tensors in each layer. The results revealed that the calculated NQR parameters were not similar for various nuclei; hence, the electrostatic environment of AlPNTs was not equivalent in length in both nanotube models. A quick look at the results revealed that the values of C_Q (^{27}Al) in the first layer of all armchair and zigzag models were largest among other layers. The Al atoms placed at the first layer played a significant role in determining the electronic behavior of nanotubes. The electrostatic environment of the first layer was stronger than that of the other layers.

The comparison of results showed that in all adsorption models from the first to the second layers C_Q values significantly decreased from original values. A significant reduction was also observed for C_Q of model D of undoped and Ge-doped (4,4) armchair and model B of undoped and model C of Ge-doped (6,0) zigzag AlPNTs.

Table 3. NQR parameters of ^{13}Al atoms for O_2 adsorption on pristine and Ge-doped (4,4) armchair models of AlPNTs.

Layers	A Model				B Model				C Model				D Model			
	Undoped		Ge-doped		Undoped		Ge-doped		Undoped		Ge-doped		Undoped		Ge-doped	
	C_Q	η	C_Q	η	C_Q	η	C_Q	η	C_Q	η	C_Q	η	C_Q	η	C_Q	η
Layer1	33.01	0.38	33.06	0.39	32.98	0.39	33.16	0.39	33.09	0.39	33.06	0.39	32.85	0.38	33.06	0.45
Layer2	20.20	0.09	20.61	0.09	20.19	0.08	20.22	0.08	20.08	0.08	20.12	0.07	19.75	0.05	19.40	0.09
Layer3	19.77	0.08	20.23	0.06	19.34	0.07	19.80	0.07	20.30	0.10	19.84	0.07	19.80	0.08	17.80	0.06
Layer4	20.19	0.11	17.58	0.10	22.63	0.25	22.00	0.19	21.39	0.14	19.33	0.07	18.42	0.13	20.11	0.11

Table 4. NQR parameters of ^{13}Al atoms for O_2 adsorption on pristine and Ge-doped (6,0) zigzag models of AlPNTs.

Layers	A Model				B Model				C Model				D Model			
	Undoped		Ge-doped		Undoped		Ge-doped		Undoped		Ge-doped		Undoped		Ge-doped	
	C_Q	η	C_Q	η	C_Q	η	C_Q	η	C_Q	η	C_Q	η	C_Q	η	C_Q	η
Layer1	33.22	0.41	33.30	0.41	33.11	0.40	33.40	0.42	33.48	0.42	33.23	1 0.4	33.59	0.43	33.06	0.41
Layer2	20.02	0.06	19.49	0.03	17.29	0.07	21.53	0.12	22.03	0.14	18.76	0.09	24.00	0.24	20.30	0.25
Layer3	20.45	0.15	19.31	0.03	19.86	0.24	19.00	0.40	20.16	0.17	19.26	0.03	20.19	0.25	19.78	0.10
Layer4	18.19	0.18	20.90	0.08	24.18	0.16	21.68	0.10	20.53	0.06	20.52	0.06	20.79	0.07	21.85	0.11

4. Conclusion

The aim of this work was to study the effects of Ge doping and O_2 adsorption on structural parameters, HOMO/LUMO orbital, quantum parameters, and NQR parameters of (4,4) armchair and (6,0) zigzag models of AlPNTs. The structural and electrical properties were investigated by density function theory, at B3LYP level of theory, and 6-31G(d) base set using the Gaussian 03 set of programs. The structural parameters revealed that the bond lengths (Al–P) of the neighborhood of doping and adsorbing sites increased and bond angles (Al–P–Al) decreased. The adsorption energy of O_2 for undoped models was in the range of –26.16 to –33.90 kcal/mol and for Ge-doped models it is in the range of –29.95 to –38.22 kcal/mol. The results showed that the E_{ads} of model C of Ge-doped (4,4) armchair and model B of Ge-doped (6,0) zigzag AlPNTs configurations was –38.22 and –31.91 kcal/mol, respectively, which are thermodynamically the most stable, and in both of them the distance of O_2 with nanotubes was 1.504 Å. Due to adsorption of O_2 on the surface of nanotubes whether in undoped (A–D) models or in Ge-doped AlPNTs E_{gap} was significantly reduced. The results revealed that the values of C_Q (^{27}Al) were largest in the first layer of all models compared with those of other layers. NQR results showed that in all adsorption models C_Q values from the first to the second layers significantly decreased from original values, which in turn indicated reduction of the electrostatic property.

Acknowledgment

We would like to thank the Computer Center at Malayer University for their kind support in performing some of the computations.

References

[1] Iijima, S. *Nature* **1991**, *354*, 2148–2152.

[2] Blase, X.; Rubio, A.; Louie, S. G.; Cohen, M. L. *Euro. Phys. Let.* **1994**, *28*, 335–340.

[3] Chopra, N. G.; Chopra, N. G.; Luyken, R. J.; Cherrey, K.; Crespi, V. H.; Cohen, M. L.; Louie, S. G.; Zettl, A. *Science* **1995**, *269*, 966–967.

[4] Zhang, D.; Zhang, R. Q. *Chem. Phys. Let.* **2003**, *371*, 426–432.

[5] Zhao, M.; Xia, Y.; Tan, Z.; Liu, X.; Li, F.; Huang, B.; Ji, Y.; Zhang, D.; Mei, L. *Chem. Phys. Let.* **2004**, *389*, 160–165.

[6] Xu, H. Y.; Liu, Z.; Zhang, X. T.; Hark, S. K. *Appl. Phys. Let.* **2007**, *90*, 113105–131058.

[7] Mirzaei, M.; Mirzaei, M. *Solid State Sci.* **2011**, *13*, 244–250.

[8] Song, W.; Ni, M.; Lu, J.; Gao, Z.; Nagase, S.; Yu, D.; Ye, H.; Zhan, X. *J. Mol. Struct. (THEOCHEM)* **2005**, *730*, 121–124.

[9] Thapa, R.; Saha, B.; Das, N. S.; Maiti, U. N.; Chattopadhyay, K. K. *Appl. Surf. Sci.* **2010**, *256*, 3988–3992.

[10] Lin, T. W.; Choi, S. Y.; Kim, Y. H.; Green, M. L. H. *Carbon* **2010**, *48*, 2401–2408.

[11] Cui, X. Y.; Yang, B. S.; Wu, H. S. *J. Mol. Struct. (THEOCHEM)* **2010**, *941*, 144–149.

[12] Montoya, A.; Gil, J. O.; Mondragón, F.; Truong, T. N. *Fuel Chem. Divis. Prep.* **2002**, *47*, 424–427.

[13] De Almeida, J. M.; Kar, T.; Piquini, P. *Phys. Lett. A.* **2010**, *374*, 877–881.

[14] Rafati, A. A.; Hashemianzadeh, S. M.; Bolboli Nojini, Z. J. *J. Colloid. Inter. Sci.* **2009**, *336*, 1–12.

[15] Ahmadi, A.; Beheshtian, J.; Hadipour, N. L. *Physica E.* **2011**, *43*, 1717–1719.

[16] Baei, T.; Peyghan, A. A.; Bagheri, Z. *Chin. Chem. Let.* **2012**, *23*, 965–968.

[17] Dong, Q.; Li, X. M.; Tian, W. Q.; Huang, X. R.; Sun, C. C. *J. Mol. Struct. (THEOCHEM)* **2010**, *948*, 83–92.

[18] Wang, H.; Liu, W.; Zhao, J. X. *Physica B* **2012**, *407*, 4238–4243.

[19] Khorrampour, R.; Esrafili, M.; Hadipour, N. L. *Physica E* **2009**, *41*, 1373–1378.

[20] Ahmadi, A.; Beheshtian, J.; Hadipour, N. L. *Physica E* **2011**, *43*, 1717–1719.

[21] Ahmadi, A.; Kamfiroozi, M.; Beheshtian, J.; Hadipour, N. L. *Struct. Chem.* **2011**, *22*, 1261–1265.

[22] Garg, A.; Vijayaraghavan, V.; Mahapatra, S. S.; Tai, K.; Wong, C. H. *Exp. Sys. Appl.* **2014**, *41*, 1389–1399.

[23] Jiao, Y.; Du, A.; Zhu, Z.; Rudolph, V.; Smith, S. C. *J. Mate. Chem.* **2010**, *20*, 10426–10430.

[24] Beheshtian, J.; Kamfiroozi, M.; Bagheri, Z.; Ahmadi, A. *Physica E* **2011**, *44*, 546–549.

[25] Baei, M. T.; Soltani, A. R.; Moradi, A. V.; Lemeski, E. T. *Comp. Theor. Chem.* **2011**, *970*, 30–35.

[26] Fernandez, E. M.; Eglitis, R. I.; Borstel, G.; Balbas, L.C. *Comp. Mat. Sci.* **2007**, *39*, 587–592.

[27] Barberio, M.; Barone, P.; Bonanno, A.; Xu, F. *Super. Micr.* **2009**, *46*, 365–368.

[28] Silva-Tapia, A. B.; Carmona, X. G.; Radovic, L. R. *Carbon* **2012**, *50*, 1152–1162.

[29] Chen, Y.; Hu, C. L.; Li, J. Q.; Jia, G. X.; Zhang, Y. F. *Chem. Phys. Let.* **2007**, *449*, 149–154.

[30] Baei, M. T.; Ahmadi Peyghan, A.; Bagheri, Z. *Chin. Chem. Let.* **2012**, *23*, 965–968.

[31] Dong, Q.; Li, X. M.; Tian, W. Q.; Huang, X. R.; Sun, C. C. *J. Mol. Struct. (THEOCHEM)* **2010**, *948*, 83–92.

[32] Chen, Y.; Hu, C. L.; Li, J. Q.; Jia, G. X.; Zhang, Y. F. *Chem. Phy. Let.* **2007**, *449*, 149–154.

[33] Liang, R. L.; Zhang, Y.; Zhang, J. M. *App. Sur. Sci.* **2010**, *257*, 282–289.

[34] Rezaei-Sameti, M. *Physica E* **2012**, *44*, 1770–1775.

[35] Rezaei-Sameti, M. *Physica B* **2012**, *407*, 3717–3721.

[36] Rezaei-Sameti, M. *Physica B* **2012**, *407*, 22–26.

[37] Rezaei-Sameti, M. *Quant. Mat.* **2013**, *2*, 1–5.

[38] Lee, C.; Yang, W.; Parr, R. G. *Phys. Rev. B* **1988**, *37*, 785–789.

[39] Frisch, M. J.; Trucks, G. W.; Schlegel, H. B.; Scuseria, G. E.; Robb, M. A.; Cheeseman, J.; Zakrzewski, V. G.; Montgomery, J. A.; Stratmann, R. E.; Burant, J. C.; et al. GAUSSIAN 03, **2003.**

[40] Ditchfield, R.; Hehre, W. J.; Pople, J. A. *J. Chem. Phys.* **1972**, *54*, 724–728.

[41] Baei, M. T.; Moghimi, M.; Torabi, P.; Varasteh Moradi, A. *Comp. Theo. Chem.* **2011**, *972*, 14–19.

[42] Chattaraj, P. K.; Sarkar, U.; Roy, D. R. *Chem. Rev.* **2006**, *106*, 2065–2091.

[43] Pyykkö, P. *Mol. Phys.* **2001**, *99*, 1617–1629.

[44] Vaara, J. *Phys. Chem. Chem. Phys.* **2007**, *9*, 5399–5418.

[45] Chen, H.; Ray, A. K. *J. Nanopart. Res.* **2013**, *15*, 1907–1921.

[46] Chen, H.; Ray, A. K. *Eur. Phys. J. B.* **2013**, *86*, 293–294.